Degradation and debromination of bromophenols using a free-base porphyrin and metalloporphyrins as photosensitizers under conditions of visible light irradiation in the absence and presence of humic substances

Qianqian Zhu [a], Mami Igarashi [a], Masahide Sasaki [b], Takafumi Miyamoto [a], Ritsu Kodama [a], Masami Fukushima [a,*]

[a] Laboratory of Chemical Resources, Division of Sustainable Resources Engineering, Faculty of Engineering, Hokkaido University, Sapporo 060-6828, Japan
[b] National Institute of Advanced Industrial Science and Technology (AIST), 2-17-2-1 Tsukisamu-Higashi, Toyohira-ku, Sapporo 062-8517, Japan

ARTICLE INFO

ABSTRACT

The photodegradation and debromination of 2,4,6-tribromophenol (TrBP) and tetrabromobisphenol A (TBBPA) were investigated in the presence of a free-base porphyrin and metalloporphyrins as photosensitizers under conditions of visible light irradiation. Among the photosensitizers, 5,10,15,20-tetrakis(N-methylpyridinium-4-yl)porphyrin (H$_2$TMPyP) and Zn(II)-tetrakis(N-methylpyridinium-4-yl)porphyrin (ZnTMPyP) were effective in the photodegradation of bromophenols. In particular, 96% of the debromination was achieved in the case of the ZnTMPyP photosensitization system for TBBPA after 24 h of irradiation. ESR spectra with a spin-trapping reagent indicated that singlet oxygen ($^1O_2$) was the major photo-induced reactive oxygen species. The presence of humic substances and natural organic matter, which are common components in landfill leachates, inhibited the photodegradation of TrBP via competitive oxidation by $^1O_2$ when ZnTMPyP was used as a photosensitizer. The presence of humic acids, which contained higher levels of electron-rich moieties like aromatic carbons, strongly inhibited the photodegradation of TrBP. TrBP and TBBPA were ultimately decomposed to organic acids, such as maleic and fumaric acids, as evidenced by LC/TOF-MS analysis. Thus, the photoirradiation of H$_2$TMPyP and ZnTMPyP can induce $^1O_2$ generation, which is effective in the photodegradation and debromination of TrBP and TBBPA.

© 2015 Elsevier B.V. All rights reserved.

1. Introduction

Bromophenols are widely utilized as additives for flame retardants in a large volume of resins and polyester polymers [1]. Among various bromophenols, tetrabromobisphenol A (TBBPA) is the most widely used of the brominated flame retardants (BFRs) in the world, representing about 60% of the total BFR market [2,3], while 2,4,6-tribromophenol (TrBP) is the most widely produced bromophenol [4]. The widespread utilization of TBBPA and TrBP leads to their ubiquitous occurrence in the environment [5,6]. Relatively high levels of bromophenols have been detected in landfill leachates, especially from landfills that involve the disposal of electronic wastes [7]. Bromophenols have also been reported to have endocrine disruption effects, and have been detected in mammalian tissue even in human blood and milk [8,9]. Therefore, it is necessary to develop effective techniques to degrade bromophenols to remove it from contaminated water.

Past methods for the oxidative degradation of bromophenols are based on the use of metal oxides [10,11], biomimetic catalytic systems using iron(III)-porphyrins and an oxygen donor [12–16], permanganate [17,18] and photocatalysts [19–26]. In particular, the photodegradation of bromophenols was performed with direct UV irradiation, UV/Fenton degradation, UV–vis/BiOBr and related reactions [19,21,25,27,28]. Metal oxides, such as TiO$_2$, had widely been used as photocatalysts for the degradation of chlorophenols [29,30]. However, the effective wavelength range for accomplishing this is mainly in UV region. Because UV light accounts for only a small portion (∼5%) of the sunlight spectrum in comparison to

the visible region (~45%), photocatalysts that can respond in the visible region have attracted much attention. Compared with inorganic photocatalysts, organometallic photosensitizers can function in the visible region [31].

Metalloporphyrins are widely used as photosensitizers in photodynamic therapy and dye sensitized solar cells because of their advantages such as being non-toxic and their excellent photo-response in visible light [32–35]. It has been reported that oxygen molecule was activated by the photosensitization of free-base porphyrins and metalloporphyrins to form singlet oxygen ($^1O_2$), which is a reactive oxygen species (ROS) [36–41]. The $^1O_2$ from the photosensitized porphyrins was applied to the oxidation of organic substrates, such as furfuryl alcohol [36] and 1,3-diphenylisobenzofuran [37]. Iron(III)-porphyrins are regarded to be biomimetic catalysts, since they mimic the active center of certain oxidative enzymes, such as ligninase and peroxidases [42]. Although iron(III)-porphyrin/$KHSO_5$ catalytic systems exhibit excellent performance for the oxidative degradation of bromophenols [13–16], the efficiency of debromination is quite low [15,43]. However, much less is known regarding the photodegradation and debromination of bromophenols by photosensitized processes in the presence of free-base porphyrins and metalloporphyrins. Although the oxidation of TBBPA by $^1O_2$ from the photosensitization of methylene blue and rose bengal has been reported, debromination has not been observed [44].

On one hand, humic substances (HSs) and natural organic matter (NOM) are major components in landfill leachates, which can function as inhibitors in the oxidation of bromophenols [13–16]. However, the influence of HSs and NOM on the photodegradation of bromophenols in the presence of free-base porphyrins and metalloporphyrins as photosensitizers have not been investigated in detail.

In the present study, the photodegradation and debromination of TBBPA and TrBP in the presence of free-base porphyrin and metalloporphyrins as photosensitizers were examined. To elucidate the oxidation characteristics of bromophenols, the oxidation products were analyzed by LC/TOF-MS. In addition, the influence of various HSs and NOM on the efficiencies of bromophenol photodegradation was investigated, and the photo-induced $^1O_2$, which serves as a ROS, was detected by ESR using a spin-trapping agent.

2. Materials and methods

2.1. Chemicals

Shinshinotsu soil humic acid (SHA) was extracted from a Shinshinotsu peat soil, as described in a previous report [45]. The reference samples for humic (HAs), fulvic (FAs) acids and NOM samples from Elliott soil (ESHA and ESFA), Pahokee peat (PPHA and PPFA), Waskish peat (WPHA and WPFA), Suwannee river (SRNOM and SRFA) and Nordic lake (NRNOM, NAHA and NAFA) were obtained from the International Humic Substances Society (St. Paul, MN, USA). The Mn(III)-tetrakis(N-methylpyridinium-4-yl) porphyrin (MnTMPyP) and Zn(II)-tetrakis(N-methylpyridinium-4-yl) porphyrin (ZnTMPyP) were provided as tetrachloride salts (Sigma–Aldrich). A tetra(p-toluenesulfonate) salt of 5,10,15,20-tetrakis(N-methylpyridinium-4-yl) porphyrin (H_2TMPyP) was purchased from Sigma–Aldrich. TBBPA and TrBP were purchased from Tokyo Chemical Industry. 2,6-Dibromo-p-benzoquinone (DBQ) [46] and the tetrachloride salt of Fe(III)-tetrakis(N-methylpyridinium-4-yl) porphyrin (FeTMPyP) [47] were synthesized, as described in previous reports. Spin-trapping agents, 2,2,6,6-tetramethyl-4-piperidone hydrochloride (TMPD) and N-tert-butyl-α-phenylnitrone (PBN), were purchased from Labotec and Sigma–Aldrich, respectively.

2.2. Degradation tests for bromophenols

A 20 mL aliquot of a 0.02 M phosphate buffer (pH 6–8) or acetate buffer (pH 4) was placed in a 100-mL Erlenmeyer flask, which was made from Pyrex® glass that can transmit light at wavelengths above 360 nm. A 100 μL aliquot of 0.01 M TrBP or TBBPA in acetonitrile and 500 μL aliquot of 200 μM of the aqueous stock solution of porphyrin derivatives were then added to the buffer. The flask was then allowed to shake at 25 °C in an incubator under irradiation using light-emitting diode (LED) lamps, in which the intensity of the irradiated light was measured to be 16 W m^{-2} and the range of wavelength for the emitted light was 400–800 nm (Fig S1). After irradiating, the concentrations of the remaining TrBP and TBBPA were determined using HPLC with UV detection. Separation was accomplished with a COSMOSIL 5C18-AR-II column (4.6 × 250 mm). The mobile phase was a mixture of methanol and water, acidified with aqueous 0.08% H_3PO_4 (76:24 in volume). The flow rate of the eluent and the detection wavelength were set at 1.0 mL min^{-1} and at 220 nm, respectively. The released Br$^-$ was analyzed by ion chromatography (Dionex ICS-90 type, Thermo Scientific) using an AS-12 type anion-exchange column (Thermo Scientific) for separation. The mobile phase was an aqueous mixture of 2.7 mM Na_2CO_3 and 0.3 mM $NaHCO_3$, and the flow rate was set at 1.5 mL min^{-1}.

2.3. ESR spectra

ESR spectra were recorded at room temperature using a quartz flat cell on a JEOL JES-TE300 ESR spectrometer. Due to the lower intensity of the LED-derived light, the generation of $^1O_2$ may be slow. To observe the more rapid generation of $^1O_2$, ESR spectra were recorded under irradiation with a Xe lamp (532 W m^{-2}, λ > 370 nm). The aqueous solutions, which contained H_2TMPyP or metalloporphyrins with the spin-trapping reagents in the absence or presence of NaN_3 were irradiated with a Xe lamp for several minutes at room temperature. The samples were then quickly placed in a quartz flat cell and measured under the following conditions: microwave power 10 mW; microwave frequency 9.43 GHz; magnetic field 335 mT; field amplitude ± 2.5 mT; modulation amplitude 0.100 mT, modulation width 25 μT; sweep time 2 min; and a time constant of 0.03 s.

2.4. Analysis of oxidation products

The oxidation products in the reaction mixtures were analyzed by LC/TOF-MS. An Agilent 1100HPLC instrument with a C18 Zorbax Extend column (2.1 mm × 100 mm, 1.8 μm particle size) for pre-separation was coupled to the detector by a Bruker micrOTOF MS at the Open Facility of Hokkaido University (Sapporo, Japan). The gradient elution using mobile phase consisted of acetonitrile/ammonium formate (10 mM), which changed from 1:99 to 90:10 for 35 min and kept for 2 min, and then returned in 2 min to 1:99, and held for 5 min for re-equilibration of the column. The flow rate was set at 0.2 mL min^{-1}, and a 10 μL volume of the sample was injected.

3. Results and discussions

3.1. Influence of photosensitizers on bromophenol degradation

Four types of a free-base porphyrin and metalloporphyrins were tested as photosensitizers for the degradation of TrBP. As shown in Fig. 1, no TrBP degradation was observed under light irradiation alone (2 h). In the presence of a free-base porphyrin (H_2TMPyP), a relatively higher percent of TrBP degradation was achieved for 2 h of irradiation. Among the metalloporphyrins, the highest percent
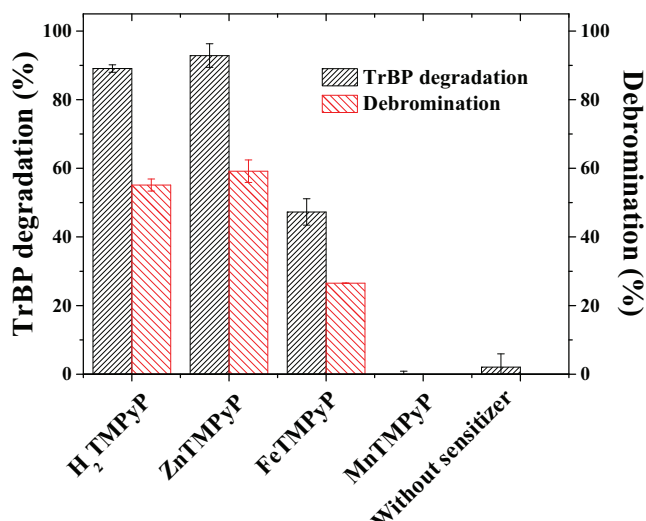
Fig. 1. Influence of a free-base porphyrin and metalloporphyrins on the photodegradation of TrBP. Reaction conditions: $[TrBP]_0$ 50 μM; $[Sensitizers]_0$ 5 μM; pH 6; irradiation time 2 h.

TrBP degradation was observed in the presence of ZnTMPyP. Only 50% of TrBP was degraded in the presence of FeTMPyP, while no degradation occurred with MnTMPyP.

A long-lived triplet state is required for the higher quantum yield of ROS in a porphyrin sensitizer. As described in a previous report [48], a long-lived triplet state and relatively higher triplet quantum yield are observed in metalloporphyrins containing diamagnetic metals, while a much shorter triplet state is observed in metalloporphyrins with paramagnetic transition metals. This suggests that the photodegradation and debromination of TrBP can be enhanced in the presence of metalloporphyrins, when they are coordinated with diamagnetic metals. Thus, ZnTMPyP, with a diamagnetic center metal, showed a higher catalytic activity for the photodegradation of TrBP.

3.2. Effect of O_2 on the photodegradation of bromophenols

ROSs may serve as oxidants in degrading bromophenols. To confirm whether O_2 is required or not, photoirradiation tests were performed under air-purging or N_2-purging. As shown in Fig. 2, 95% of the TrBP was degraded after a 3-h irradiation period and 68% of Br^- was released in the systems with and without air-purging. However, no photodegradation of TrBP was observed when N_2-purging was used. These results indicate that O_2 is required for the photodegradation of TrBP. However, the turnover frequency (TOF) for the photodegradation of TrBP with air-purging (20.2 h^{-1}) was nearly the same as that without purging (20.6 h^{-1}). These results show that the dissolved O_2 in aqueous solution (water-solubility of O_2, 1.3 mM at 25 °C) is sufficient for the photodegradation of TrBP in the presence of ZnTMPyP.

TBBPA degradation was also examined under light irradiation in the presence of ZnTMPyP (Fig. 3). The TOF for the photodegradation of TBBPA (29.2 h^{-1}) was higher than that for an Fe(III)-porphyrin/KHSO$_5$ system (6.4 h^{-1}) [49], and 90% of the TBBPA was degraded after 4 h of irradiation. In addition, 44% of Br^- was released from TBBPA in 4 h of irradiation. After a 24-h irradiation period, all of the TBBPA was degraded and 96% of debromination was achieved. The debromination of TBBPA is difficult to achieve in iron(III)-porphyrin/KHSO$_5$ catalytic systems [15,43,44], in which the percent debromination is estimated to be below 30%. Thus, a photodegradation system using a ZnTMPyP photosensitizer is a more efficient process for the oxidative
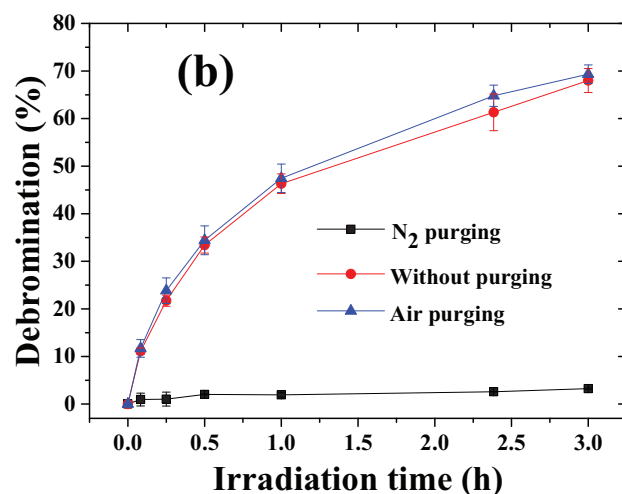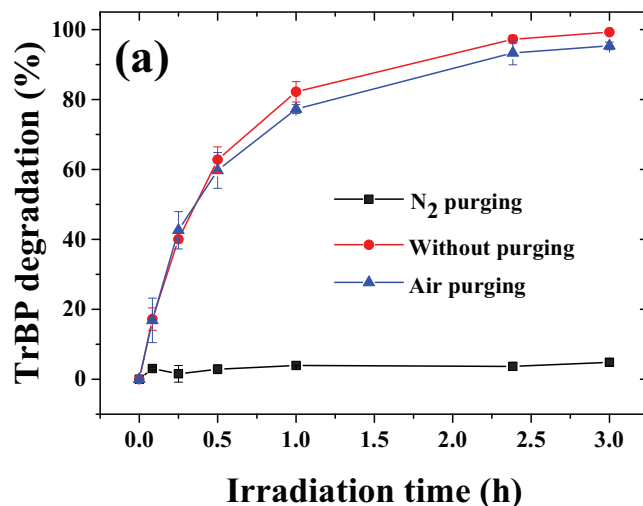

Fig. 2. Influence of air-purging and N_2-purging on the photo-degradation of TrBP. Reaction conditions: $[TrBP]_0$ 50 μM; $[ZnTMPyP]_0$ 5 μM; pH 6.
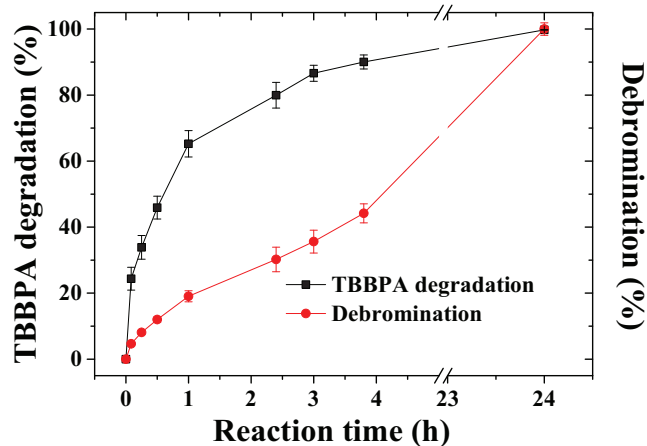

Fig. 3. Kinetic curves for the photodegradation of TBBPA. Reaction conditions: $[TBBPA]_0$ 50 μM; $[ZnTMPyP]_0$ 5 μM; pH 8.
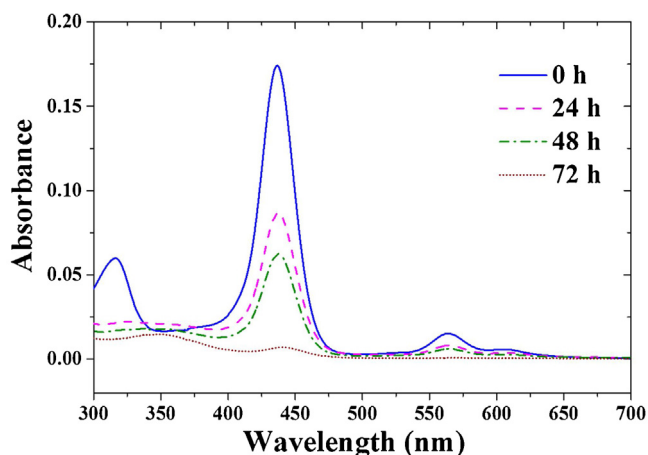
Fig. 4. Variations in UV–vis absorption spectra of reaction mixture containing ZnTMPyP and TrBP during irradiation. Reaction conditions: $[TrBP]_0$ 50 μM; $[ZnTMPyP]_0$ 5 μM; pH 8.

debromination of bromophenols than the systems for combining iron(III)-porphyrins with $KHSO_5$ as an oxygen donor.

The durability of ZnTMPyP was tested in the presence of TrBP. Fig. 4 shows the variations in UV–vis absorption spectra of the reaction mixture containing TrBP and ZnTMPyP during irradiation. The absorption maximum at 486 and 564 nm, which can be assigned as the Soret and Q bands of ZnTMPyP, respectively, decreased with an increase in the irradiation time. After irradiating for 72 h, the absorption peaks for the Soret and Q bands of ZnTMPyP disappeared, indicating that ZnTMPyP was bleached. This result can be attributed to the self-degradation of ZnTMPyP by the generated $^1O_2$. However, approximately 50% of the ZnTMPyP was not degraded after a 24-h period of irradiation, where 96% of debromination was observed in the case of TBBPA (Fig. 3).

3.3. Effect of ZnTMPyP concentration

The effect of the concentration of ZnTMPyP on bromophenol photodegradation is shown in Fig. 5. The percent of TrBP photodegradation linearly increased with increasing ZnTMPyP concentration from 0.1 to 5 μM for a 1 h period of irradiation and

then remained constant with further increases in the concentration of ZnTMPyP. The percent TBBPA degradation also showed the similar trend to the case of TrBP. The turnover numbers (TONs) for the photodegradation and debromination of TrBP and TBBPA were estimated by dividing the concentrations of the bromophenols degraded by ZnTMPyP (0.1 μM) as follows: photodegradation, 48.5 for TrBP and 23.5 TBBPA; debromination, 51.6 for TrBP and 55.8 for TBBPA. The significant effects of the concentration of ZnTMPyP on bromophenol degradation suggest that ZnTMPyP is required as a photosensitizer in generating ROS.

3.4. ROSs detection by ESR

It has been reported that $^1O_2$ and the superoxide radical anion ($O_2^{\bullet-}$) are major ROSs that are generated as a result of the photosensitization of free-base porphyrins and Zn-porphyrins [38,50]. To elucidate the major ROS that can contribute to the photodegradation of bromophenol, ESR measurements in the presence of spin-trapping agent were conducted. TMPD was employed as a spin-trapping agent for $^1O_2$, and PBN was used for trapping $O_2^{\bullet-}$ and $HO^\bullet$ radicals. Spin trapping of $^1O_2$ was based on the oxidation of diamagnetic TMPD by $^1O_2$ to yield paramagnetic 2,2,6,6-tetramethyl-4-piperidone-1-oxyl (TMPD-O) [51]. After irradiation with a 500 W Xe lamp ($\lambda > 370$ nm), the ESR spectrum showed three major signals with the same intensity and a hyperfine coupling constant, $A_N = 1.600$ mT, which can be assigned as TMPD-O. The intensity of the TMPD-O peak increased with increasing irradiation time (Fig. 6). No signal was observed in the absence of light irradiation or ZnTMPyP. After the addition of NaN_3, which is widely used as a $^1O_2$ quencher, a significant decrease in the TMPD-O signal was observed in the presence of 1 M NaN_3, while the signals disappeared when 10 M NaN_3 was present, which verifies the formation of $^1O_2$ (Fig. 7a). A TrBP degradation test was also performed in the presence of NaN_3 (Fig. 7b), and a decrease in the percent photodegradation was observed. These results show that $^1O_2$ is the major ROS that is produced during the degradation. The ESR spectra of TMPD-O in the presence of H_2TMPyP, ZnTMPyP and FeTMPyP are shown in Fig. S2. The TMPD-O signal intensity decreased in the following order: ZnTMPyP $\approx H_2TMPyP >$ FeTMPyP, indicating that each of the photosensitizers results in a different quantum yield of $^1O_2$. Although the addition of PBN was examined for the detection of $HO^\bullet$ and $O_2^{\bullet-}$ adducts, no signal was observed.
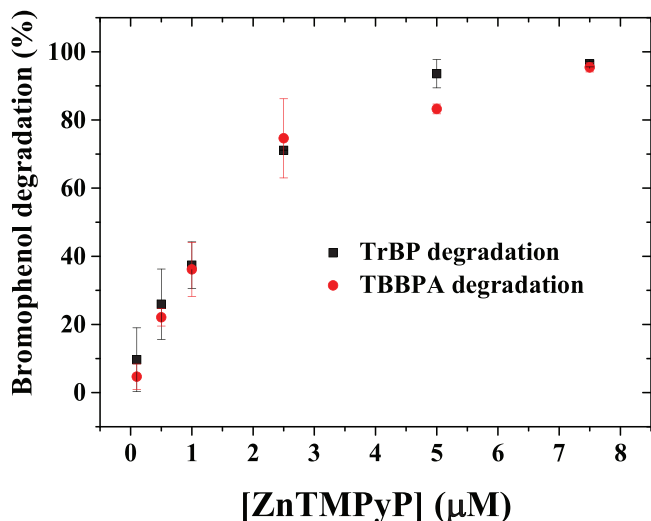

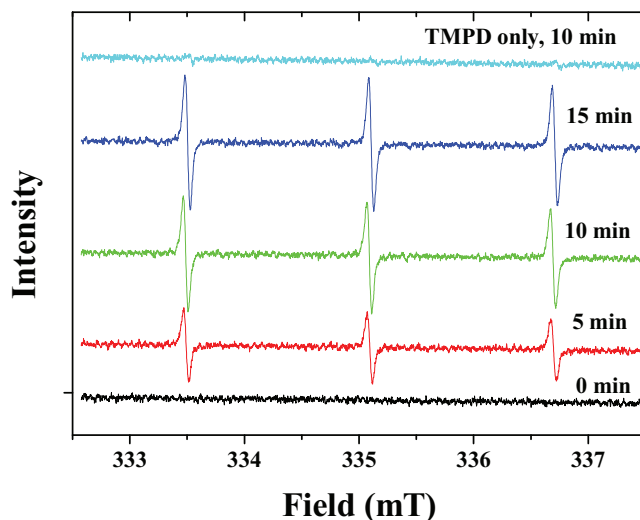**Fig. 5.** Photodegradation of TrBP (■) or TBBPA (●) under various ZnTMPyP concentrations. Reaction conditions: (1) TrBP degradation, $[TrBP]_0$ 50 μM; $[ZnTMPyP]_0$ 5 μM; pH 8, irradiation time 1 h. (2) TBBPA degradation, $[TrBP]_0$ 50 μM; $[ZnTMPyP]_0$ 5 μM; pH 8, irradiation time 2 h.

Fig. 6. ESR spectra of aqueous mixtures of ZnTMPyP and TMPD for different periods of irradiation. Reaction conditions: [ZnTMPyP] 5 μM; pH 8; [TMPD] 0.02 M.
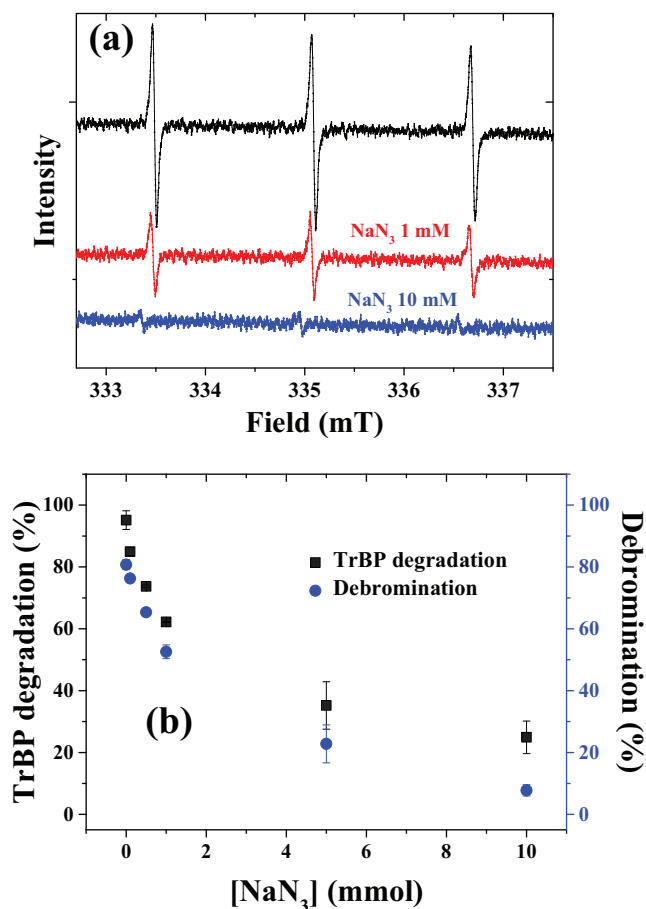
Fig. 7. Influence of NaN$_3$ on the intensity of TMPD-O adduct in ESR spectra (a) and on photodegradaion percent of TrBP (b). Reaction conditions for (a): [ZnTMPyP]$_0$ 5 μM; [TMPD] 0.02 M; pH 8; irradiation time 10 min (Xe lamp). Reaction conditions for (b): [TrBP]$_0$ 50 μM; [ZnTMPyP]$_0$ 5 μM; pH 8; irradiation time 1 h (LED lamp).

Fig. 8. Influence of pH on TrBP degradation percent (a) and debromination (b). Reaction conditions: [Bromophenol]$_0$, 50 μM, [ZnTMPyP]$_0$, 5 μM, irradiation time 2 h.

Furfuryl alcohol (FFA) is used as a ^{1}O$_2$ quencher to determine its concentration in the presence of a photosensitizer [52,53]. The percent photodegradation of FFA in the presence of H$_2$TMPyP and metalloporphyrins are shown in Fig. S3. The percent FFA degradation showed a similar trend to that for TrBP degradation (Fig. 1). These results indicate that the levels of ^{1}O$_2$ generation are dependent on the type of photosensitizer being used.

3.5. Influence of pH

Fig. 8 shows the influence of pH on the percent of photodegradation and debromination of TrBP and TBBPA. Only 13% of the TrBP was degraded at pH 4, while more than 90% of TrBP was degraded above pH 6. The percent of photodegradation of TBBPA also increased with increasing pH, and significantly increased up to 82% at pH 8. The percent debromination of TrBP and TBBPA increased with an increase in pH, and the highest levels of debromination were observed at pH 8.

The pH dependence on the photodegradation of bromophenol in the presence of ZnTMPyP may be attributed to: (i) the levels of photo-induced ^{1}O$_2$, and (ii) deprotonation of bromophenols. To analyze the levels of the generated ^{1}O$_2$, FFA was used as the quencher of ^{1}O$_2$. As shown in Fig. S4, the percent of FFA photodegradation at pH 4 was the highest, while 68–72% of the FFA was degraded in the pH range of 6–8. These results indicate that the levels of ^{1}O$_2$ generation are relatively higher in the acidic region and almost the same level at pH 6–8. The pK_a values for TrBP and TBBPA are 5.97 and 7.50, respectively, and bromophenols
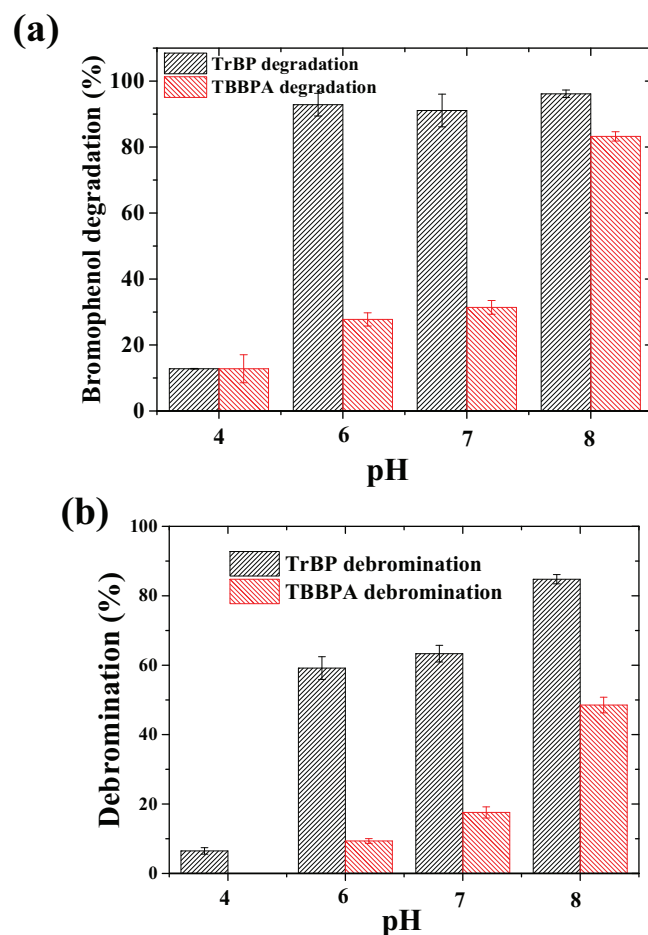
are deprotonated to form phenolate anions above these pH values. The pH dependence on photodegradation and debromination were consistent with the pK_a values of each bromophenol. Phenolate anions have the higher electron densities rather than the protonated species, and ^{1}O$_2$ is electrophilic in nature. Thus, the higher percent photodegradation of TBBPA and TrBP above the pH values for each pK_a can be attributed to the fact that the deprotonated species of bromophenols are more easily attacked by ^{1}O$_2$. This is supported by a previous report that the reaction rate constant for the oxidation of 4-chlorophenol by ^{1}O$_2$ (6.0×10^6 M^{-1} s^{-1}) is much smaller than that for the 4-chlorophenolate anion (1.9×10^8 M^{-1} s^{-1}) [54].

3.6. Influence of HSs and NOM

HSs are widely distributed in landfill leachates, which affect the solubility, mobility, decomposition rate, and fate of organic pollutants [55]. The efficiencies of bromophenol oxidation are inhibited in the presence of dissolved organic matter, such as HSs and NOM [14,16,56,57]. In the case of iron(III)-porphyrin/KHSO$_5$ catalytic systems, the degradation of bromophenol in the presence of HSs and NOM have been reported to be inhibited [13,14,16]. In the photocatalytic oxidation systems, HSs can serve as photosensitizer [58–60], while the presence of HSs sometimes inhibits the photodegradation [61,62]. Such differences in the effects of HSs and NOM on photocatalytic processes may be dependent on the variety of their structures. To investigate the influence of HSs (HAs and
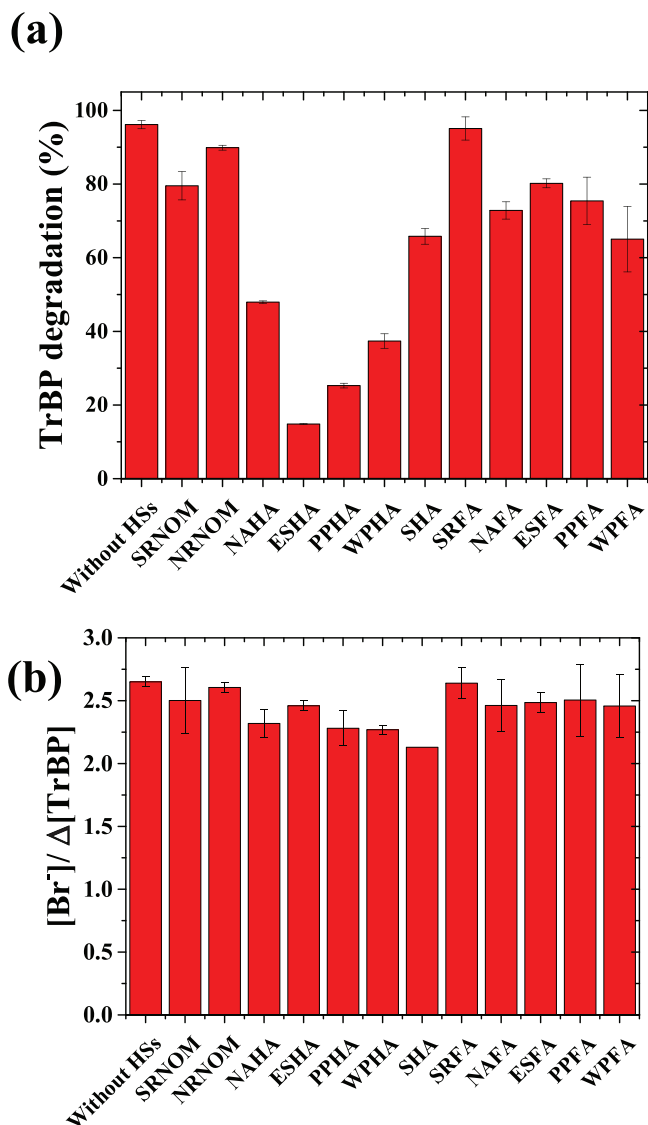
(a)

(b)

Fig. 9. Influence of HSs and NOM on the percent photodegradation of TrBP (a) and debromination (b). Reaction conditions: [TrBP]$_0$ 50 μM; [ZnTMPyP]$_0$ 5 μM; [HSs or NOM] 10 mg L^{-1}; pH 8; irradiation time 2 h.

FAs) and NOM on the photodegradation of bromophenols in the presence of ZnTMPyP, several types of HA, FA and NOM samples were examined, in which TrBP was selected as a model of a bromophenol. As shown in Fig. 9, the presence of HSs greatly inhibited the photodegradation of TrBP. The influence of the concentrations of SHA and SRFA on TrBP degradation is shown in Fig. S5. The percent TrBP degradation decreased with increasing HS concentration. These results support conclusion that the photodegradation of TrBP is inhibited in the presence of HSs. Lower levels of TrBP photodegradation were observed in the presence of ESHA and PPHA. In contrast, relatively higher levels of TrBP photodegradation were achieved in the presence of NOM and FAs. The levels for debromination remained relatively constant between HSs and NOM samples, and 2–2.5 bromine atoms were released from the degraded TrBP.

The inhibitions of TrBP oxidation in the presence of HSs and NOM can be attributed to competition between TrBP and HSs or NOM with $^1O_2$. To confirm that $^1O_2$ is consumed by HSs, ESR spectra were recorded in the presence of SRNOM and PPHA. As shown in Fig. 10, the TMPD-O signal significantly decreased in the presence of PPHA, while the presence of SRNOM had no effect on the
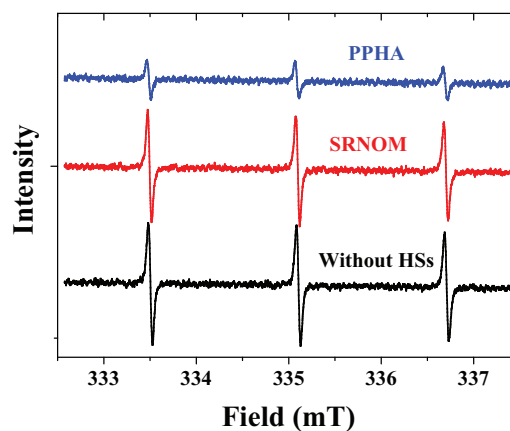

Fig. 10. ESR spectra of aqueous mixtures of ZnTMPyP, HSs and TMPD under photoirradiation. Reaction conditions: [ZnTMPyP] 5 μM; pH 8; [HSs] 50 mg L^{-1}; and [TMPD] 0.02 M; irradiation time 15 min.

signal intensity. This result shows that $^1O_2$ was consumed by PPHA. The reaction rate constant for HSs and NOM are reported to be in the range of 10^6–10^8 M^{-1} s^{-1} and these levels are dependent on the dissociation of phenols [63]. Thus, the differences in the levels of inhibition for the TrBP degradation by photo-induced $^1O_2$ in the presence of HSs and NOM may be dependent on their structural features [56]. Fig. S6 shows the relationships between the percent TrBP
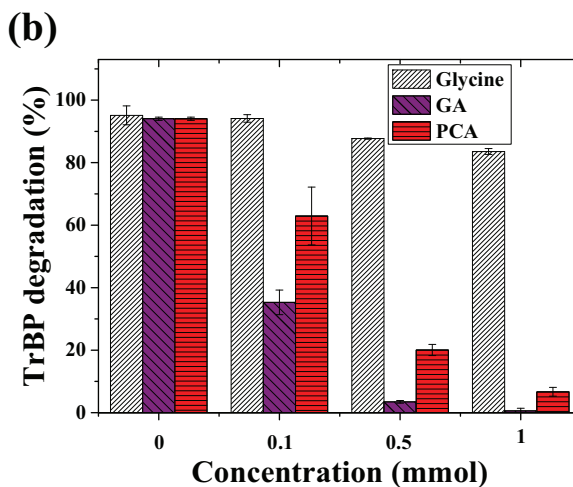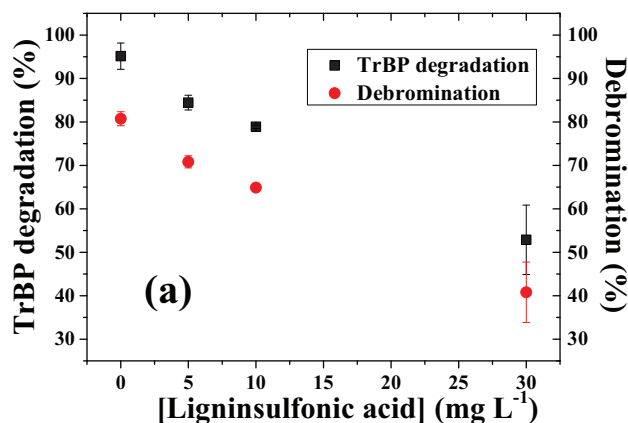

Fig. 11. Influence of structural groups in HSs, Ligninsulfonic acid (a), Glycine, Gallic acid (GA), and Protocatechuic acid (PCA) (b) on the percent photodegradation of TrBP. Reaction conditions: [TrBP]$_0$ 50 μM; [ZnTMPyP] 5 μM; pH 8; irradiation time; 1 h.
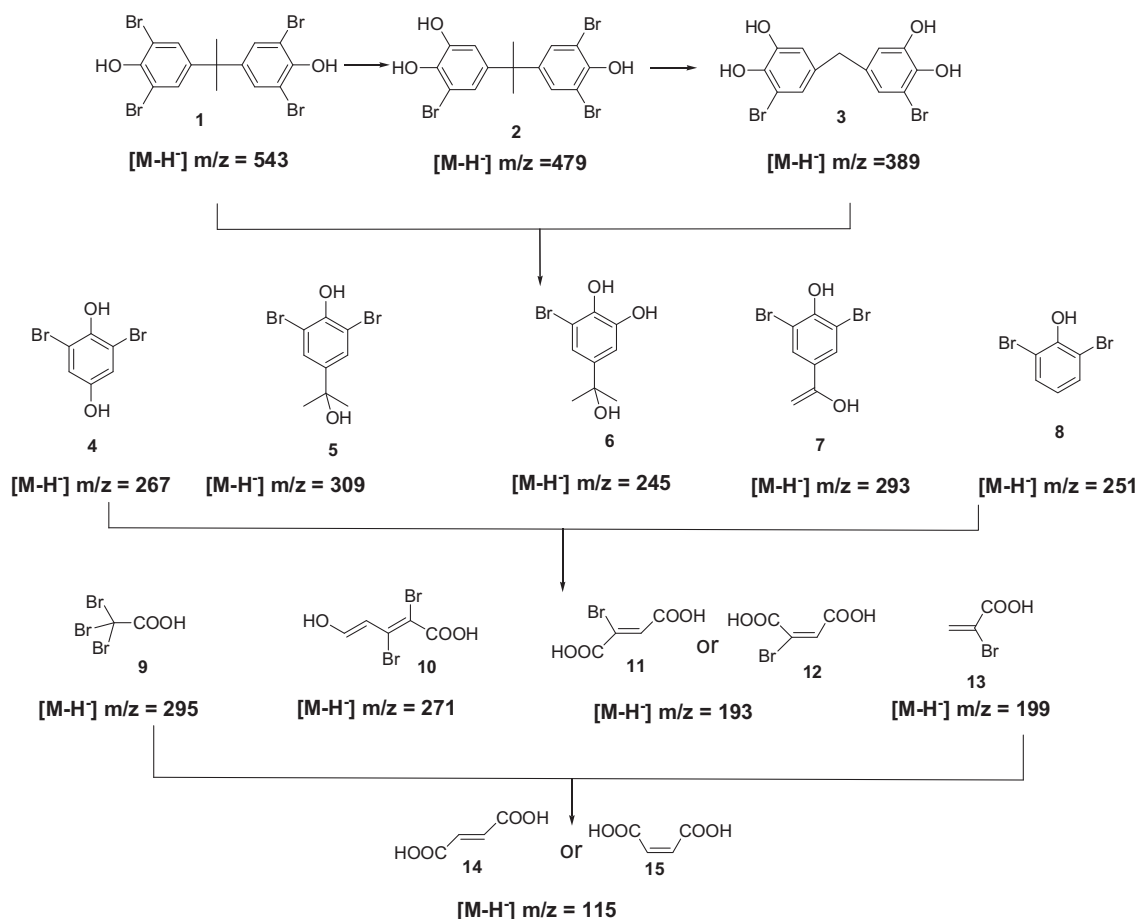
Fig. 12. Possible photodegradation pathways of TBBPA in the presence of ZnTMPyP. Oxidation products after 1 h, 4 h and 28 h of irradiation were analyzed by LC/TOF-MS.

photodegradation and the content of phenolic hydroxyl groups or aromatic carbon in HS and NOM samples. Although no correlations were clearly observed for either of these structural parameters, HAs that contained higher levels of aromatic carbon resulted in a lower percent of TrBP photodegradation.

Singlet oxygen can directly react with the electron-rich double bonds of unsaturated molecules. Lignosulfonate, gallic acid, protocatechuic acid and glycine are known to be structural components of HSs and NOM [64,65]. To elucidate the dependence on structural features, the influence of these structural parts on the photodegradation of TrBP was investigated (Fig. 11). Lignosulfonate, gallic acid and protocatechuic acid, all of which contain aromatic structures, inhibited the degradation of TrBP. However, glycine that contains no unsaturated double bonds did not inhibit. These results indicate that electron-rich moieties of HSs and NOM can serve as inhibitors for the photodegradation of TrBP.

3.7. Possible photodegradation pathway

The oxidation products from the photodegradation of bromophenols were monitored by LC/TOF-MS. Based on the detected products, the possible pathways for the photodegradation of TBBPA are proposed, as shown in Fig. 12. Scission of a β-carbon first occurs to convert compounds 1–3 into 2,6-dibromophenol derivatives (products 4–8). Subsequently, C–Br cleavage and ring-cleavage results in the formation of brominated organic acids, and these products are finally degraded to maleic (product 15) and fumaric (product 14) acids *via* debromination. In a previous report [44], the major degradation product of TBBPA by 1O2 was reported to be DBQ (product 4). In the present study, a small amount of DBQ

was detected after 1 h of irradiation period, while the majority of the detected products were ring-cleavage organic acids after 4 and 28 h of irradiation. Fig. S7 shows possible degradation pathways for TrBP, based on the oxidation products detected in the reaction mixture by LC/TOF-MS. The higher levels of debromination in the photosensitization by ZnTMPyP are consistent with the formation of organic acids without bromine, such as maleic and fumaric acids, while the mineralization of TBBPA to CO_2 was not observed in the reaction mixture after photoirradiation. However, the photo-induced $^1O_2$ in the presence of ZnTMPyP leads to higher levels of debromination and ring-cleavage to form environmental friendly organic acids.

4. Conclusion

The photodegradation and debromination of bromophenols were observed in the presence of free-base porphyrin and metalloporphyrins under visible light irradiation. Among the photosensitizers examined, higher levels of photodegradation in TrBP and TBBPA were observed in the presence of ZnTMPyP and H_2TMPyP. ESR spectra, which were recorded using a spin-trapping agent, proved that $^1O_2$ was the major ROS produced during the photodegradation. The presence of HSs and NOM affected the levels of photodegradation of TrBP *via* a competitive oxidation by $^1O_2$. Although the degree of inhibition for the degradation of TrBP was dependent on the types of HSs and NOM present, HAs that contained higher levels of electron-rich moieties (aromatic moieties) more strongly inhibited the photodegradation of TrBP. More than 95% of the debromination was achieved in the case of TBBPA after a 24-h period of irradiation, in which this is a higher level than that

for the iron(III)-porphyrin/KHSO$_5$ catalytic systems (below 30%). In conclusion, H$_2$TMPyP and ZnTMPyP enhance the generation of ^{1}O$_2$, and are effective in the photodegradation and debromination of bromophenols.

Acknowledgment

Appendix A. Supplementary data

Supplementary data associated with this article can be found, in the online version, at http://dx.doi.org/10.1016/j.apcatb.2015.10.038.

References

[1] A. Covaci, S. Harrad, M.A.-E. Abdallah, N. Ali, R.J. Law, D. Herzke, C.A. de Wit, Environ. Int. 37 (2011) 532–556.
[2] European Risk Assessment Report: 2,2′,6,6′-tetrabromo-4,4′-isopropylidenediphenol (tetrabromobisphenol-A or TBBPA-A), Part II, Human health., 2006.
[3] Scientific opinion in tetrabromobisphenol A (TBBPA) and its derivatives in food, Parma, Italy, 2011.
[4] P.D. Howe, S. Dobson, H.M. Malcolm, 2,4,6-Tribromophenol and other simple brominated phenol, World Health Organization, Geneva, 2005.
[5] A. Sjödin, D.G. Patterson, A. Bergman, Environ. Int. 29 (2003) 829–839.
[6] Y. Fujii, E. Nishimura, Y. Kato, K.H. Harada, A. Koizumi, K. Haraguchi, Environ. Int. 63 (2014) 19–25.
[7] M. Osako, Y.-J. Kim, S. Sakai, Chemosphere 57 (2004) 1571–1579.
[8] J. Legler, A. Brouwer, Environ. Int. 29 (2003) 879–885.
[9] S. Strack, T. Detzel, M. Wahl, B. Kuch, H.F. Krug, Chemosphere 67 (2007) S405–S411.
[10] K. Lin, W. Liu, J. Gan, Environ. Sci. Technol. 43 (2009) 4480–4486.
[11] L. Zhou, L. Ji, P.-C. Ma, Y. Shao, H. Zhang, W. Gao, Y. Li, J. Hazard. Mater. 265 (2014) 104–114.
[12] Y. Ding, L. Zhu, N. Wang, H. Tang, Appl. Catal. B: Environ. 129 (2013) 153–162.
[13] Q. Zhu, Y. Mizutani, S. Maeno, R. Nishimoto, T. Miyamoto, M. Fukushima, J. Environ. Sci. Heal. A 48 (2013) 1593–1601.
[14] Q. Zhu, S. Maeno, M. Sasaki, T. Miyamoto, M. Fukushima, Appl. Catal. B: Environ. 163 (2015) 459–466.
[15] Q. Zhu, Y. Mizutani, S. Maeno, M. Fukushima, Molecules 18 (2013) 5360–5372.
[16] Q. Zhu, S. Maeno, R. Nishimoto, T. Miyamoto, M. Fukushima, J. Mol. Catal. A: Chem. 385 (2014) 31–37.
[17] S.Y. Pang, J. Jiang, Y. Gao, Y. Zhou, X. Huangfu, Y. Liu, J. Ma, Environ. Sci. Technol. 48 (2014) 615–623.
[18] J. Du, B. Sun, J. Zhang, X. Guan, Environ. Sci. Technol. 46 (2012) 8860–8867.
[19] P. Miró, A. Arques, A.M. Amat, M.L. Marin, M.A. Miranda, Appl. Catal. B: Environ. 140–141 (2013) 412–418.
[20] K. Yu, S. Yang, C. Liu, H. Chen, H. Li, C. Sun, S.a. Boyd, Environ. Sci. Technol. 46 (2012) 7318–7326.
[21] J. Xu, W. Meng, Y. Zhang, L. Li, C. Guo, Appl. Catal. B: Environ. 107 (2011) 355–362.
[22] E. Díez-Mato, F.C. Cortezón-Tamarit, S. Bogialli, D. García-Fresnadillo, M.D. Marazuela, Appl. Catal. B: Environ. 160–161 (2014) 445–455.
[23] B. Gao, L. Liu, J. Liu, F. Yang, Appl. Catal. B: Environ. 147 (2014) 929–939.
[24] C. Sun, W. Chang, W. Ma, C. Chen, J. Zhao, Environ. Sci. Technol. 47 (2013) 2370–2377.
[25] Y. Zhong, X. Liang, Y. Zhong, J. Zhu, S. Zhu, P. Yuan, H. He, J. Zhang, Water Res. 46 (2012) 4633–4644.
[26] Y. Guo, L. Chen, X. Yang, F. Ma, S. Zhang, Y. Yang, Y. Guo, X. Yuan, RSC Adv. 2 (2012) 4656–4663.
[27] G.P. Anipsitakis, D.D. Dionysiou, Appl. Catal. B: Environ. 54 (2004) 155–163.
[28] B. Gao, L. Liu, J. Liu, F. Yang, Appl. Catal. B: Environ. 129 (2013) 89–97.
[29] D. Méndez, R. Vargas, C. Borrás, S. Blanco, J. Mostany, B.R. Scharifker, Appl. Catal. B: Environ. 166–167 (2015) 529–534.
[30] S. Krejčíková, L. Matějová, K. Kočí, L. Obalová, Z. Matěj, L. Čapek, O. Šolcová, Appl. Catal. B: Environ. 111–112 (2012) 119–125.
[31] M.L. Marin, L. Santos-Juanes, A. Arques, A.M. Amat, M.a. Miranda, Chem. Rev. 112 (2012) 1710–1750.
[32] C.P. Ponce, R.P. Steer, M.F. Paige, Photochem. Photobiol. Sci. 12 (2013) 1079–1085.
[33] X.-T. Zhou, H.-B. Ji, X.-J. Huang, Molecules 17 (2012) 1149–1158.
[34] J. Bernadou, B. Meunier, Chem. Commun. (1998) 2167–2173.
[35] A. Beeby, S. Fitzgerald, C.F. Stanley, J. Chem. Soc., Perkin Trans. 2 (2001) 1978–1982.
[36] H. Kim, W. Kim, Y. Mackeyev, G.-S. Lee, H.-J. Kim, T. Tachikawa, S. Hong, S. Lee, J. Kim, L.J. Wilson, T. Majima, P.J.J. Alvarez, W. Choi, J. Lee, Environ. Sci. Technol. 46 (2012) 9606–9613.
[37] L.M. Rossi, P.R. Silva, L.L.R. Vono, A.U. Fernandes, D.B. Tada, M.S. Baptista, Langmuir 24 (2008) 12534–12538.
[38] K. Ergaieg, M. Chevanne, J. Cillard, R. Seux, Sol. Energy 82 (2008) 1107–1117.
[39] D.F. Zigler, E.C. Ding, L.E. Jarocha, R.R. Khatmullin, V.M. DiPasquale, R.B. Sykes, V.F. Tarasov, M.D.E. Forbes, Photochem. Photobiol. Sci. 13 (2014) 1804–1811.
[40] W. Hiraoka, H. Honda, L.B. Feril Jr., N. Kudo, T. Kondo, Ultrason. Sonochem. 13 (2006) 535–542.
[41] Y.M. Riyad, S. Naumov, S. Schastak, J. Griebel, A. Kahnt, T. Häupl, J. Neuhaus, B. Abel, R. Hermann, J. Phys. Chem. B 118 (2014) 11646–11658.
[42] Metalloporphyrins in Catalytic Oxidations, in: F. Montanari, L. Casella (Eds.), Kluwer, Dordrecht, 1994.
[43] S. Maeno, Y. Mizutani, Q. Zhu, T. Miyamoto, M. Fukushima, H. Kuramitz, J. Environ. Sci. Heal. A 49 (2014) 981–987.
[44] S.K. Han, P. Bilski, B. Karriker, R.H. Sik, C.F. Chignell, Environ. Sci. Technol. 42 (2008) 166–172.
[45] F. Tanaka, M. Fukushima, A. Kikuchi, H. Yabuta, H. Ichikawa, K. Tatsumi, Chemosphere 58 (2005) 1319–1326.
[46] S. Shigetatsu, M. Fukushima, S. Nagao, J. Environ. Sci. Heal. A 45 (2010) 1536–1542.
[47] T. Miyamoto, R. Nishimoto, S. Maeno, Q. Zhu, M. Fukushima, J. Mol. Catal. B: Enzym. 99 (2014) 150–155.
[48] M.C. DeRosa, R.J. Crutchley, Coordin. Chem. Rev. 233–234 (2002) 351–371.
[49] T. Miyamoto, Q. Zhu, R. Igrashi, R. Kodama, S. Maeno, M. Fukushima, J. Mol. Catal. B: Enzym. 119 (2015) 64–70.
[50] M. Hajimohammadi, F. Bahadoran, S.S.H. Davarani, N. Safari, Reac. Kinet. Mech. Cat. 99 (2010) 243–250.
[51] W. He, H.K. Kim, W.G. Wamer, D. Melka, J.H. Callahan, J.J. Yin, J. Am. Chem. Soc. 136 (2014) 750–757.
[52] F. Vargas, M.V. Hisbeth, J.K. Rojas, J. Photochem. Photobiol. A: Chem. 118 (1998) 19–23.
[53] F. Vargas, I. Martinez Volkmar, J. Sequera, H. Mendez, J. Rojas, G. Fraile, M. Velasquez, R. Medina, J. Photochem. Photobiol. B: Biol. 42 (1998) 219–225.
[54] F. al Housari, D. Vione, S. Chiron, S. Barbati, Photochem. Photobiol. Sci. 9 (2010) 78–86.
[55] lignin, Humic Substances and Coal, in: M. Hofrichter, A. Steinbüchel (Eds.), Biopolymer, Wiley-VCH, 2001, 2015.
[56] J. Brame, M. Long, Q. Li, P. Alvarez, Water Res. 60 (2014) 259–266.
[57] M. Aeschbacher, C. Graf, R.P. Schwarzenbach, M. Sander, Environ. Sci. Technol. 46 (2012) 4916–4925.
[58] M. Fukushima, K. Tatsumi, K. Morimoto, Environ. Sci. Technol. 34 (2000) 2006–2013.
[59] M. Fukushima, K. Tatsumi, K. Morimoto, Environ. Toxicol. Chem. 19 (2000) 1711–1716.
[60] M. Fukushima, K. Tatsumi, Environ. Sci. Technol. 35 (2001) 1771–1778.
[61] S. Han, R.H. Sik, A.G. Motten, C.F. Chignell, P.J. Bilski, Photochem. Photobiol. 85 (2009) 1299–1305.
[62] J.F. Leal, V.I. Esteves, E.B.H. Santos, Environ. Sci. Technol. 47 (2013) 14010–14017.
[63] K.S. Golanoski, S. Fang, R. Del Vecchio, N.V. Blough, Environ. Sci. Technol. 46 (2012) 3912–3920.
[64] M. Fukushima, K. Furubayashi, N. Fujisawa, M. Takeuchi, T. Komai, K. Ootsuka, M. Yamamoto, Y. Kawabe, S. Horiya, J. Anal. Appl. Pyrol. 91 (2011) 323–331.
[65] H. Iwai, M. Fukushima, M. Yamamoto, T. Komai, Y. Kawabe, J. Anal. Appl. Pyrol. 99 (2013) 9–15.